

# Assessment of the Effect of Current Non-Uniformity on the ITER Nb<sub>3</sub>Sn Good Joint Short Sample DC Performance

L. Savoldi Richard, P. Bruzzone, N. Mitchell, P. L. Ribani, and R. Zanino

**Abstract**—The DC performance of the so-called Good Joint Nb<sub>3</sub>Sn Short Sample conductor, measured in the SULTAN facility in 1999 with a progressively reduced (chopped) joint length, became worse as the joint became shorter. In this paper we present the analysis of those tests using the THELMA code. The results confirm quantitatively that the loss of performance was due to increasingly unbalanced current distribution. Once the unbalance due to the joint is properly modeled, the performance of the conductor can be fitted using the same extra longitudinal strain in the critical current scaling, proportional to the electromagnetic load but independent of the joint length.

**Index Terms**—Fusion reactors, modeling, superconducting magnets, testing.

## I. INTRODUCTION

**A**LONG the path towards the construction of the superconducting magnets for the International Thermonuclear Experimental Reactor (ITER), it is presently foreseen to test the conductor performance in dedicated full-size short-sample tests in the SULTAN facility. Several samples of this type, e.g., the so-called Good Joint (GJ) short sample considered here [1], were already tested in the past [2], [3]. For two of them, the GJ and the Toroidal Field Model Coil Full Size Joint Sample [4], the test of DC performance of the corresponding long conductors wound in a coil was also performed [5], [6]. Unfortunately, it has not been possible so far to demonstrate the representativity of the short sample performance for the conductor-in-coil performance [7], [8]. Compared to expectations based on the isolated (single) strand, both short samples and coils show indeed degradation, which can be well fitted in a uniform current analysis by assuming an extra longitudinal strain  $\varepsilon_{\text{extra}}$  depending on the electromagnetic load. However,  $\varepsilon_{\text{extra}}$  turns out to be different in the sample and in the coil [7], [8].

Manuscript received August 29, 2006. This work, supported by the European Communities under the contract of Association between EURATOM/ENEA, and by the Italian Ministry for Education, University and Research (MIUR), was carried out within the framework of the European Fusion Development Agreement. The views and opinions expressed herein do not necessarily reflect those of the European Commission.

R. Zanino and L. Savoldi Richard are with Dipartimento di Energetica, Politecnico, Torino, Italy (e-mail: roberto.zanino@polito.it).

P. Bruzzone is with EPFL-CRPP, Villigen, Switzerland.

N. Mitchell is with ITER IT, Naka, Japan.

P. L. Ribani is with Dipartimento di Ingegneria Elettrica, Universita' di Bologna, Italy.

Color versions of one or more of the figures in this paper are available online at <http://ieeexplore.ieee.org>.

Digital Object Identifier 10.1109/TASC.2007.899039

For both sample and coil, the analysis performed so far contains simplifying assumptions, which should be carefully reconsidered. Among those assumptions, we concentrate here on the effects of current non-uniformity on the GJ sample DC performance. Concerning the simplifying assumptions behind  $\varepsilon_{\text{extra}}$ , the need and possible scope of a more detailed thermo-mechanical model of the Nb<sub>3</sub>Sn cable should also be considered, as already albeit preliminarily discussed elsewhere [9].

The GJ sample was tested with progressively reduced (chopped) joint length. In [8] the analysis of the GJ DC tests with the original (full) joint length was performed assuming a uniform current distribution on the cross section. Here we analyse quantitatively the GJ conductor DC performance, measured at different joint lengths, using the THELMA code [10], which can model current non-uniformity.

## II. EXPERIMENTAL SETUP

The GJ short sample was assembled with two Nb<sub>3</sub>Sn cable-in-conduit conductors (CICC), leftover from the winding of the fourth layer of the ITER CSMC [11], using the VAC strand and an Incoloy 908 jacket. The GJ conductor was tested for DC performance in the SULTAN facility at Villigen PSI, Switzerland, in 1999. Three different test campaigns were performed, with a progressively reduced joint length (from the original  $L_{\text{Joint}} = 400$  mm, down to  $L_{\text{Joint}} = 320$  mm and eventually to  $L_{\text{Joint}} = 280$  mm) [1], to investigate the effect of current distribution on the conductor performance.

The setup of the experiment is schematically reproduced in Fig. 1. The sample was tested in vertical position, with He inlet (at  $\sim 1$  MPa and 4.5 K) at the bottom. The two conductor sections (“legs”) came from the same cable length, but while leg A was simply a straight section, leg B was bent and re-straightened to simulate the mechanical loads applied during the react-and-transfer coil manufacturing process.

The joint and the upper terminations are manufactured in the same way: after the removal of jacket, outer wraps and sub-cable wraps from the sides to be connected, the compacted cables are soldered to the Cu saddle modular elements. The joint is then closed into a steel box.

The experimental results show that the conductor DC performance was strongly affected by joint length (the shorter the joint, the worse the performance) [1], [12] and anyway lower than expected from the strand performance. Both issues were qualitatively explained at the time of the test as an effect of the increasing current non-uniformity at decreasing joint length, which could not be effectively redistributed because of sub-

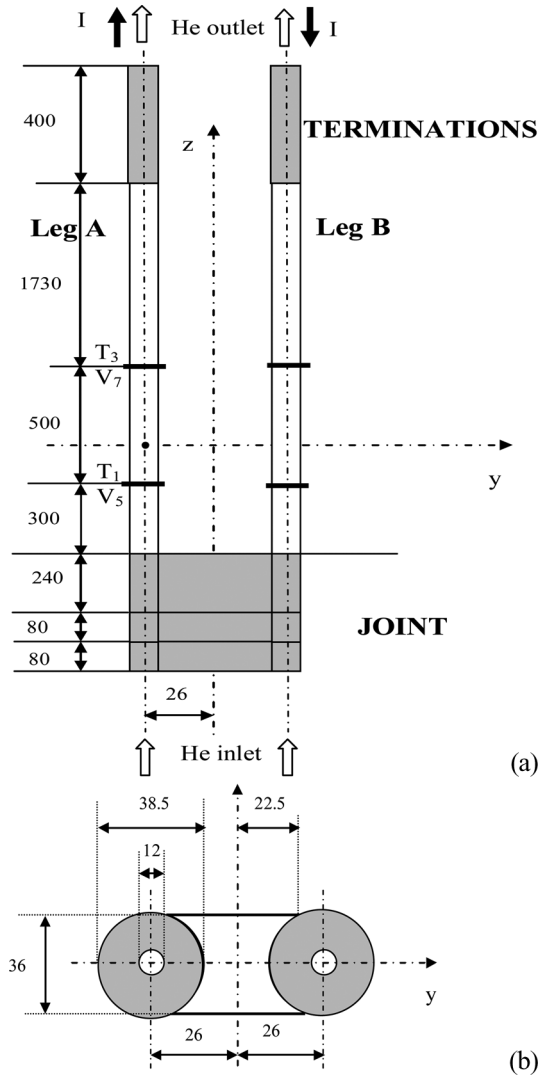


Fig. 1. Schematic view of the GJ sample: (a) longitudinal view, (b) cross section. Tx=thermometer, Vx=voltage tap. Lengths quoted in mm.

cable wraps and of the short distance between the joint and the beginning of the high field region. Here, the additional important contribution to performance degradation related to the electromagnetic load on the conductor will also be included.

### III. THELMA SIMULATION SETUP

#### A. Cable

The electromagnetic model of the cable, which is implemented in the THELMA code, is described in [10]. The current distribution among the strands is calculated by means of a distributed parameter model. In the present study, we model six cable elements (CE), corresponding to the last-but-one cabling stage (petals), so that all the strands in a petal are supposed to carry the same current, which is a function of the axial coordinate ( $z$ ) and of time ( $t$ ). The geometrical parameters of the cable are taken from [13], except for the petal twist pitch, which was assumed equal to 500 mm instead of the nominal 420 mm in view of the experimental evidence from [1]. The transverse conductance per unit length between two

adjacent petals is  $4 \times 10^5$  S/m, taken from the measurements [12]. The transverse conductance between two non-adjacent petals is considered negligible. The usual power law relation  $E = E_C(J/J_C)^n$  is utilized for the  $E - J$  characteristics of the superconducting (SC) material ( $J$  is the current density in the SC material,  $E_C = 10 \mu\text{V/m}$ ). The critical current density  $J_C$  interpolative scaling law and the  $n$ -value depend on the temperature  $T$ , on the modulus of the magnetic field  $B$  and on the longitudinal uniaxial strain  $\varepsilon$  as shown in [14], [15]. For the VAC strand we compute  $J_C = 631$  A/mm<sup>2</sup> at 4.2 K, 12 T and zero strain, fully consistent with the average  $J_C$  of the short sample conductor [13]

For the generic ( $i$ -th) CE, the uniaxial strain  $\varepsilon_i$  is supposed to depend on the local transverse electromagnetic load [5], [16]

$$\varepsilon_i(z, t) = \varepsilon_{th} + k_\varepsilon I_i(z, t) B_i(z, t) \quad (1)$$

where  $\varepsilon_{th}$  is the thermal strain,  $I_i$  and  $B_i$  are the current and magnetic field in the CE, respectively.  $k_\varepsilon$  is a constant to be determined, which is used to fit the measured critical current  $I_C$ .

From a 0D analysis of the GJ conductor DC test with the original (long) joint [8], which was carried out under the hypothesis of uniform current distribution, we derive  $\varepsilon_{th} = -0.34\%$ , and  $k_\varepsilon = -2.7 \times 10^{-8} \text{ T}^{-1} \text{ A}^{-1}$ . While in [8] (1) was based on the average magnetic field computed on the cable cross section, here we apply (1) *locally* to each petal. Thus the magnetic field  $B_i$  is computed on the respective petal axis, while the current  $I_i$  is that of each CE (because of this,  $k_\varepsilon$  is multiplied by a factor of 6 with respect to the value in [8])

#### B. Joint and Termination

The complete model of the termination/joint which is implemented in the THELMA code is described in [17]. The distribution of the current density in the termination/joint region is calculated by means of an equivalent lumped parameter network. In the present study, only resistive effects are considered. The contact resistance between the CEs and the saddle is calculated from the geometry of the CEs, assuming a value of the distributed contact resistance between CE and saddle, which roughly reproduces the measured joint resistance of  $\sim 2$  n $\Omega$  at 10 T and  $\sim 50$  kA.

Consistently with [8], we model here only the current distribution in Leg A of the sample, assuming an equipotential surface at the joint mid-plane (and at the upper termination boundary as well); the contribution of Leg B to the magnetic field is included.

#### C. Scenarios

Three  $I_C$  tests at the background field of 10 T and temperature  $T_1 \sim 7.2\text{--}7.3$  K (see Fig. 1), at the beginning of the  $I_C$  ramp have been selected, which have  $\sim$  the same Lorentz load: E0202003 (nominal  $L_{\text{Joint}} = 400$  mm), E0604009 (chopped  $L_{\text{Joint}} = 320$  mm), E1905003 (chopped  $L_{\text{Joint}} = 240$  mm). The thermal-hydraulic boundary conditions for our analysis are fixed He inlet temperature (assumed equal to the measured  $T_1$  value) and pressure, and fixed outlet pressure, such as to reproduce a mass flow rate of  $\sim 3.5$  g/s. The central channel was blocked in the shortest joint test ( $L_{\text{Joint}} = 240$  mm) and in the

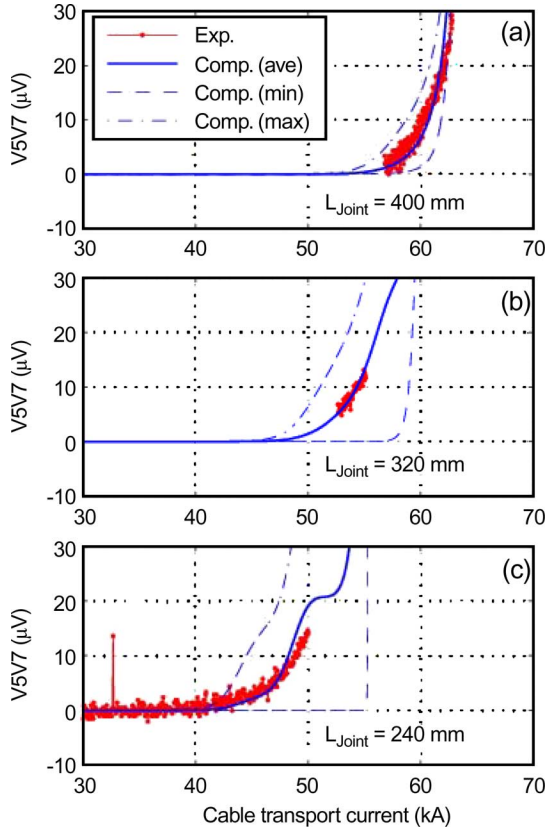


Fig. 2. Experimental (symbols) and computed average (solid) voltage evolution  $V_{5V7}$  for the different joint lengths. The computed maximum (dashed) and minimum (dash-dotted) voltage are also reported, see text.

respective simulation. The total transport current at the equipotential joint/termination surfaces is imposed.

#### IV. SIMULATION RESULTS AND COMPARISON WITH THE EXPERIMENT

The computed results are reported in Fig. 2 in terms of voltage-current (V-I) characteristics. Different CEs show different voltage evolutions, because they carry different currents and redistribution is hindered by the sub-cable wraps (see below). For the purpose of the comparison with the experiment, we consider the computed resistive voltage between V5 and V7 (see Fig. 1), averaged over the 6 petals. In some cases the full V-I characteristic was not recorded, so that the voltage offset has been chosen somewhat arbitrarily. The agreement of the simulations with the measured voltage is very good (within  $\sim 1$  kA) for all joint lengths. The slope is somewhat overestimated, but this is due to the assumption  $n_{\text{petal}} = n_{\text{strand}}$ . Since the strain recipe (1) is the same for the three simulations, the degradation in conductor performance with the progressive joint chopping (computed  $I_C$  @  $10 \mu\text{V}/\text{m} \sim 59.5$  kA, 52.6 kA and 47 kA, respectively) is confirmed to be due only to the increasing current non-uniformity induced by the joint.

The computed evolution of the current unbalance among the petals (more-or-less uniform *along* the conductor, because of the low inter-petal conductance) is reported in Fig. 3 for the different joint lengths. It is shown that the current unbalance  $I_{\text{petal}}/I_{\text{ave}}$  is in the range  $\sim 70$ – $130\%$  in the case of the shortest

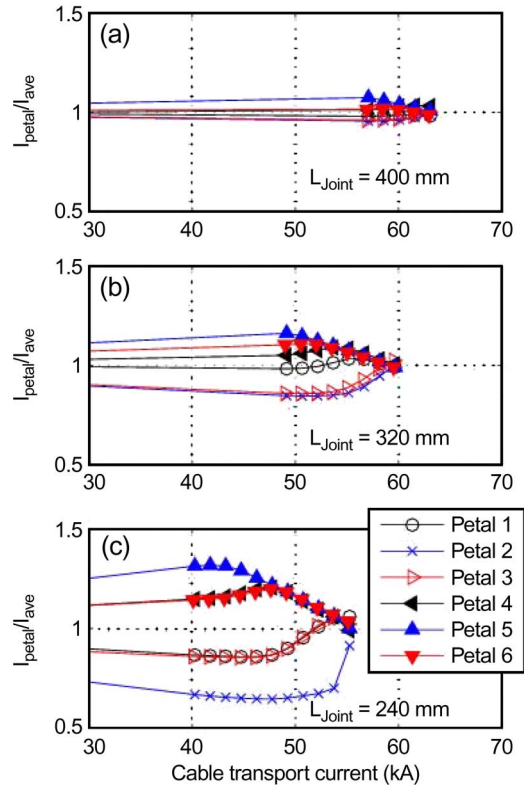


Fig. 3. Computed current unbalance in the petals for the different joint lengths.

joint, while the current is almost uniform in the case of the original (unchopped) joint.

Again due to the low value of the transverse conductance between the CEs, the redistribution of the current takes place in the joint/termination region. Before the current sharing regime is reached, the current repartition among the CEs, develops towards the resistive distribution due to the termination/joint contact resistances with the petals. The current sharing regime starts in this case before the resistive distribution is reached. In Fig. 3(c) the mechanism of current redistribution to adjacent petals can be well observed: the petal #5 is the first to approach the critical condition, because it carries the highest current in view of the longest contact (lowest resistance) with the joint saddle, see Fig. 4.  $I_5$  redistributes to the adjacent petals #4 and 6 and petals #1 and 3 are involved only eventually, while the farthest petal (#2) is the slowest to react. (Note that, in Fig. 3(b), petal #3 follows this time petal #2, which is again a consequence of contact distribution, see Fig. 4). The current redistribution to adjacent petals causes also a change of slope in the computed V-I characteristic, see Fig. 2(c), which is unfortunately impossible to confirm experimentally, because data acquisition was interrupted early in this case. This could also be related, however, to the assumed values for inter-petal conductance.

#### V. CONCLUSIONS AND PERSPECTIVE

The THELMA analysis of the effects of current non-uniformity on the DC performance of the GJ conductor has quantitatively confirmed the previous qualitative suggestion that the reduction of the performance with the chopped joint is an effect

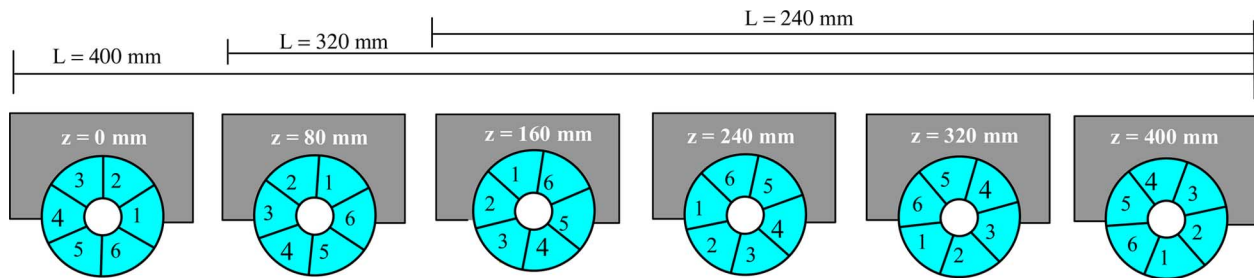


Fig. 4. Cable geometry in the joint as modeled by THELMA: cross sections at different axial locations  $z$ , with the respective position of the different petals (#1 to #6). The dark grey section indicates the joint saddle. The joint ends at  $z = 400$  mm where the conductor starts.

of the current unbalance in the cable. The V-I characteristics of Leg A measured at the same field and total Lorentz force, but for different joint lengths, have been well fitted using locally the same longitudinal strain recipe and suitably modeling the joint length reduction. This confirms the results of previous analysis based on the uniform current assumption [8], showing that the short sample performance degradation with respect to the strand is not related to current non-uniformity but can be correlated with the transverse electromagnetic load (and also with cycling effects—to be discussed elsewhere). This analysis additionally indicates that the discrepancy between the sample and the conductor-in-coil DC performance cannot be due, in this case at least, to current non-uniformity effects in the sample. A thermo-mechanical model of the cable, more physically based than (1), is being developed [9] to address this remaining open issue.

#### REFERENCES

- [1] "Development of an Improved Joint for ITER CS1 Conductor and Joint Test in SULTAN," compiled by P. Bruzzone, Villigen, December 1999.
- [2] Y. Takahashi *et al.*, "Performance of joints in the CS model coil and application to the full size ITER coils," *IEEE Trans. Appl. Supercond.*, vol. 14, pp. 1523–1526, 2004.
- [3] K. Seo, "Electromagnetic properties of lap-joint and its influences on the conductor test data," *IEEE Trans. Appl. Supercond.*, vol. 16, pp. 856–859, 2006.
- [4] D. Ciazynski, J.-L. Duchateau, T. Schild, and A. Fuchs, "Test results and analysis of two European full-size conductor samples for ITER," *IEEE Trans. Appl. Supercond.*, vol. 10, pp. 1058–1061, 2000.
- [5] R. Zanino, N. Mitchell, and L. Savoldi, "Analysis and interpretation of the full set (2000–2002) of Tcs tests in conductor 1 A of the ITER central solenoid model coil," *Cryogenics*, vol. 43, pp. 179–197, 2003.
- [6] L. Savoldi *et al.*, "First measurement of the current sharing temperature at 80 kA in the ITER Toroidal Field Model Coil (TFMC)," *IEEE Trans. Appl. Supercond.*, vol. 12, pp. 635–638, 2002.
- [7] R. Zanino, D. Ciazynski, N. Mitchell, and L. S. Richard, "Coupled mechanical-electromagnetic-thermal-hydraulic effects in Nb<sub>3</sub>Sn Cable-in-Conduit conductors for ITER," *Supercond. Sci. Technol.*, vol. 18, pp. S376–S382, 2005.
- [8] L. S. Richard, N. Mitchell, and R. Zanino, "From short sample to coil DC superconductor performance: ITER Central Solenoid Model Coil (CSMC) vs. Good Joint (GJ) sample," *IEEE Trans. Appl. Supercond.*, vol. 16, pp. 799–802, 2006.
- [9] R. Zanino, D. P. Boso, M. Lefik, L. S. Richard, and B. A. Schrefler, "A novel thermo-mechanical approach to DC performance modelling of Nb<sub>3</sub>Sn superconducting cable-in-conduit conductors in ITER perspective," presented at the MEM06, UK, July 3–5, 2006, Durham University, unpublished.
- [10] M. Ciotti, A. Nijhuis, P. L. Ribani, L. S. Richard, and R. Zanino, "THELMA code electromagnetic model of ITER superconducting cables and application to the ENEA stability experiment," *Supercond. Sci. Technol.*, vol. 19, pp. 987–997, 2006.
- [11] R. Jayakumar *et al.*, "Fabrication of ITER central solenoid model coil inner module," *IEEE Trans. Appl. Supercond.*, vol. 7, pp. 981–984, 1997.
- [12] P. Bruzzone, A. M. Fuchs, G. Vecsey, and E. Zapretalina, "Test results for the high field conductor of the ITER central solenoid model coil," *Adv. Cryo. Eng.*, vol. 45, pp. 729–736, 2000.
- [13] Database of CSMC and CS Insert JAERI memo 12-046, March 2000.
- [14] D. M. J. Taylor and D. P. Hampshire, "The scaling law for the strain dependence of the critical current density in Nb<sub>3</sub>Sn superconducting wires," *Supercond. Sci. Technol.*, vol. 18, pp. 241–252, 2005.
- [15] D. M. J. Taylor and D. P. Hampshire, "Relationship between the n-value and critical current in Nb<sub>3</sub>Sn superconducting wires exhibiting intrinsic and ex-trinsic behaviour," *Supercond. Sci. Technol.*, vol. 18, pp. S297–S302, 2005.
- [16] N. Mitchell, "Mechanical and magnetic load effects in Nb<sub>3</sub>Sn cable-in-conduit conductors," *Cryogenics*, vol. 43, pp. 255–270, 2003.
- [17] F. Bellina, P. Bettini, and F. Trevisan, "Electromagnetic analysis of superconducting cables and joints in transient regime," *IEEE Trans. Appl. Supercond.*, vol. 14, pp. 1356–1359, 2004.